

Fig. 8. Effect of substrate thickness on impedance characteristics for TM_{21} and TM_{31} modes.

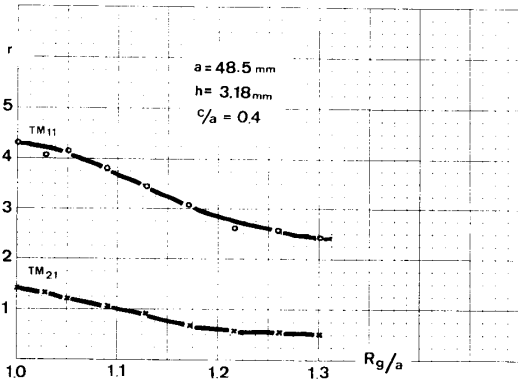


Fig. 9. Resonant resistance versus ground plane diameter for TM_{11} and TM_{21} modes.

simple correction factors to existing equations describing antenna frequency to enable a precise definition of the resonant frequency of microstrip patch antennas.

The impedance characteristics for higher modes were also presented. These characteristics are necessary to find the probe location for the best matching condition for each desired mode. They are also useful for determining the proper feed configuration for adequate mode separation. A simple method of cancelling spurious modes by means of grounding post was proposed, the position of which can be determined from the impedance characteristics of the particular mode.

The numerical analysis of finite ground plane effect on the wall admittance was recently presented by Bhattacharyya [5] and agree with the presented characteristics. A successful theoretical analysis of the input impedance dependence on the feed location has not been done so far.

APPENDIX

The input impedance of a resonator (antenna) is equal to

$$z = jx + \frac{r}{1 + jy} \tag{4}$$

where

- x coupling probe reactance (normalized to 50 Ω)
- r resistance at resonance (normalized to 50 Ω)
- $y = Q \left(\frac{f}{f_0} - \frac{f_0}{f} \right) \cong 2Q \frac{\Delta f}{f_0}$ —normalized detuning,
- $\Delta f = f - f_0$, and f_0 —cavity resonant frequency.

The input reflection coefficient is given by

$$\Gamma = \frac{z - 1}{z + 1} = \frac{(r - 1 - xy) + j(x - y)}{(r + 1 - xy) + j(x + y)} \tag{5}$$

The resonant frequency of the antenna (f'_0) is for the minimum reflection loss $|\Gamma|$, given by

$$|\Gamma| = \sqrt{\frac{(r - 1 - xy)^2 + (x - y)^2}{(r + 1 - xy)^2 + (x + y)^2}} \tag{6}$$

which occurs when the derivative of $|\Gamma|$ equals zero and can be calculated from

$$\frac{d|\Gamma|}{dy} = \sqrt{\frac{x^2 + (r + 1)^2 - 2rxy + y^2(x^2 + 1)}{x^2 + (r - 1)^2 - 2rxy + y^2(x^2 + 1)}} \cdot \frac{4r^2x - 4ry(x^2 + 1)}{M^2} \tag{7}$$

where $M = x^2 + (r + 1)^2 - 2rxy + y^2(x^2 + 1)$.

The expression under the square root sign cannot be zero since M has no roots. Thus the condition for lowest reflection loss, i.e., $d|\Gamma|/y = 0$, at $f = f'_0$, is fulfilled for

$$y' = y(f'_0) = \frac{x}{1 + x^2} \cdot r \tag{8}$$

which gives

$$|\Gamma|_{\min} = \left| \frac{r - 1 - x^2}{r + 1 + x^2} \right| \tag{9}$$

and for $r = 1 + x^2$, it reduces to zero indicating a perfect match.

REFERENCES

- [1] I. J. Bahl and P. Bhartia, *Microstrip Antennas*. Dedham, MA: Artech House, 1980.
- [2] W. C. Chew and J. A. Kong, "Effect of fringing fields on the capacitance of circular microstrip disc," *IEEE Trans. Microwave Theory Tech.*, vol. MTT-28, pp. 98-104, Feb. 1980.
- [3] K. R. Carver, "Microstrip antenna technology," *IEEE Trans. Antennas Propagat.*, vol. AP-29, pp. 2-24, Jan. 1981.
- [4] R. W. Dearnley and A. R. F. Barel, "A broad-band transmission line model for a rectangular microstrip antenna," *IEEE Trans. Antennas Propagat.*, vol. 37, pp. 6-15, Jan. 1989.
- [5] A. Bhattacharyya, "Finite ground plane effects on the radiation patterns of rectangular microstrip antenna," presented at Symp. Antenna Technol. and Appl. Electromagn. ANTEM-88, Aug. 10-12, Winnipeg, Canada.

A Simple Dual-Band Corrugated Horn with Low Cross Polarization

K. SUDHAKAR RAO, MEMBER, IEEE

Abstract—A simplified design for dual-band corrugated conical horns with low cross-polarization characteristics is discussed. Measured results of the bread-board horn show that cross-polar levels of better than -34 dB and return loss of better than 28 dB have been realized over the designed frequency bands.

Manuscript received November 30, 1988; revised June 8, 1989. This work was supported by the Department of Communication, Canada, and Spar under a joint development program SDP-86-005.

The author is with the Satellite and Aerospace Division, Spar Aerospace Ltd., 21025 Trans Canada Highway, Ste.-Anne-de-Bellevue, PQ, Canada H9X 3R2.

IEEE Log Number 9035047.

I. INTRODUCTION

There has been a considerable interest for the past several years in the development of dual-band corrugated conical horns for satellite and terrestrial communications. A high degree of polarization purity over two discrete and widely separated frequency bands has been the requirement for satellites with a common antenna for downlink and uplink communications. Dual-depth corrugated horns which utilize alternating corrugation depths to optimize the performance over two discrete bands have been developed earlier [1]–[3]. These horns require a greater number of corrugations per wavelength in comparison to the conventional corrugated horns, and are difficult to fabricate, particularly at high frequencies. Another method of broad-banding the horn performance is by using ring-loaded corrugations [4], [5], which is also quite cumbersome from a manufacturing point of view.

A simplified design for the wide-band corrugated horn is presented here using single depth corrugations. The horn is developed as a feed for an offset Cassegrain antenna employing a hyperbolic subreflector and a parabolic main reflector. The depth of the corrugations near the throat section of the horn are varied in order to optimize the horn performance in terms of cross-polarization fields and impedance match over two discrete frequency bands. Further, a TE_{11} to HE_{11} mode transformer [6] is employed to improve the impedance match between the dominant mode circular and hybrid mode corrugated sections of the horn. Measured results of the bread-board horn show that peak cross-polar levels of better than -39 and -34 dB (relative to peak) have been realized for the transmit (11.79–12.09 GHz) and receive (17.39–17.69 GHz) bands, respectively. The return loss of the horn is better than 28 dB over the designed frequency bands.

II. DESIGN OF THE CORRUGATED HORN

The horn is designed to have approximately a -15 dB taper at the subreflector edge ($\Theta_c = 13^\circ$) for the low end of the transmit band. This corresponds to a -21 dB feed taper at the high end of the receive band. Such a low taper is chosen in order to minimize the feed spillover losses. Feed spillover efficiency with this design is estimated as 0.95 and 0.98 at the transmit and receive bands, respectively. The radiation characteristics of corrugated horns can be expressed in terms of a single dimensionless parameter Δ [7], Δ being the difference in wavelengths between the spherical wavefront and the plane aperture. It is related to the horn parameters as

$$\Delta = 0.5(D/\lambda) \tan(\Theta_0/2) \quad (1)$$

where D is the aperture diameter and Θ_0 is the semiflare angle of the horn. For $\Delta < 0.4$, the beamwidth is determined mainly by the aperture size (D/λ) and is therefore frequency dependent. As the value of Δ decreases, the phase center of the horn moves toward the aperture. These horns are classified as “narrow-band horns.” For horns with $\Delta > 0.75$, the beamwidth is determined mainly by the semiflare angle Θ_0 of the horn, and the phase center is near the throat of the horn. These horns provide near frequency independent performance and are termed as “wide-band horns.” Initial design is carried out with $\Delta = 1.0$ and the horn parameters are obtained as

$$D = 17.53 \text{ in, } L = 34.03 \text{ in, and } \Theta_0 = 14.4^\circ.$$

The above horn is too big and is not compatible with the dual-reflector configuration. Therefore, a narrow-band horn is designed with $\Delta = 0.2$ at the transmit band. For receive band frequencies, the value of Δ is about 0.3. A low flare angle of $\Theta_0 = 7.2^\circ$ is chosen in order to minimize reflections from the throat section. The final design has the following significant parameters:

$$D = 6.372 \text{ in, } L = 25.22 \text{ in, and } \Theta_0 = 7.2^\circ.$$

The parameter L in the above equations is the axial length of the horn from its apex.

The next design parameter is the diameter of the circular waveguide at the input of the horn. It is a compromise between improving the return loss of the waveguide and generating higher order unwanted modes that contribute to cross polarization. Fig. 1 shows the mode chart of a corrugated circular pipe with “ $2a$ ” as the diameter of the circular waveguide and $(b - a)$ as the depth of corrugations. The region of desired hybrid HE_{11} mode is shown by hatched lines. The diameter $2a$ is chosen as 0.8 in, to achieve maximum bandwidth. Corrugation depth inside the circular waveguide is chosen as 0.314λ for reasons explained later. The ratio (b/a) for this design is 1.785. The lowest and highest frequencies of the desired band are shown in Fig. 1 as discrete points. Both the frequencies are well within the hybrid HE_{11} mode region of operation. The doubly hatched region in Fig. 1 corresponds to the case when the depth of corrugations is less than $\lambda/4$. In this region both HE_{11} and surface waves propagate and the surface impedance due to corrugations becomes inductive. This region of operation is not usually preferred because of high cross-polar fields and high impedance mismatch.

Excitation of the EH_{12} mode near the throat section of the horn causes relatively high levels of cross polarization at the high end of the frequency band. The normalized radius (ka) of the horn at the position of the first slot should be less than four at the highest frequency. For this design with $a = 0.4$ in, the range of ka is $2.508 \leq ka \leq 3.765$. The depth of corrugations near the aperture should be in the range 0.25λ to 0.5λ . For low cross-polarization levels, the corrugation depth at the lowest frequency should be as close to quarterwave as possible. Choosing $d_a = 0.256$ in, the range of (d_a/λ) within the required band is

$$0.255 \leq (d_a/\lambda) \leq 0.383.$$

For low flare angle horns ($\Theta_0 < 12^\circ$), it has been a common practice to use at least four corrugations per wavelength at highest frequency. For small ka values, the above criterion will avoid increased cross polarization which occurs when wider slots are used [8]. Therefore, pitch of the corrugation(s) is chosen as 0.164 in, which corresponds to 4.07 and 6.11 corrugations per wavelength at 17.692 and 11.785 GHz, respectively. Also, the corrugations should be as thin as possible in order to achieve good performance of the horn. Choosing the thickness (t) of the corrugations as one quarter of the slot width (w), the parameters of the corrugations are obtained as

$$t = 0.033 \text{ in and } w = 0.131 \text{ in.}$$

In order to improve the impedance match between the TE_{11} mode in the circular pipe and the HE_{11} mode in the corrugated pipe, the slots near the throat of the horn are designed to be slightly less than one-half wavelength deep at highest frequency [9]. This is due to the fact that with half-wavelength deep corrugations, the corrugated surface acts electrically as a plane conducting wall. Depth of the corrugations near the throat d_t is selected as 0.314 in ($0.47 \lambda_H$). Also, the depth of the corrugations is gradually tapered over $2 \lambda_L$ axial length (from the throat) from 0.314 to 0.256 in. Mismatch near the throat section is further minimized by first using a semiflare angle of 3.6° and later using 7.2° .

An input section with a corrugated transformer is designed for matching the TE_{11} mode impedance to the HE_{11} mode impedance of the horn. A two-section transformer with eight corrugations is designed by frequency scaling the design data of Dragone and Legg [6] by a factor of 1.63. The ratio of the lowest frequency to the cut-off frequency of the circular waveguide (f_L/f_C) is 1.3512. The input section and the throat section (where depth of successive corrugations

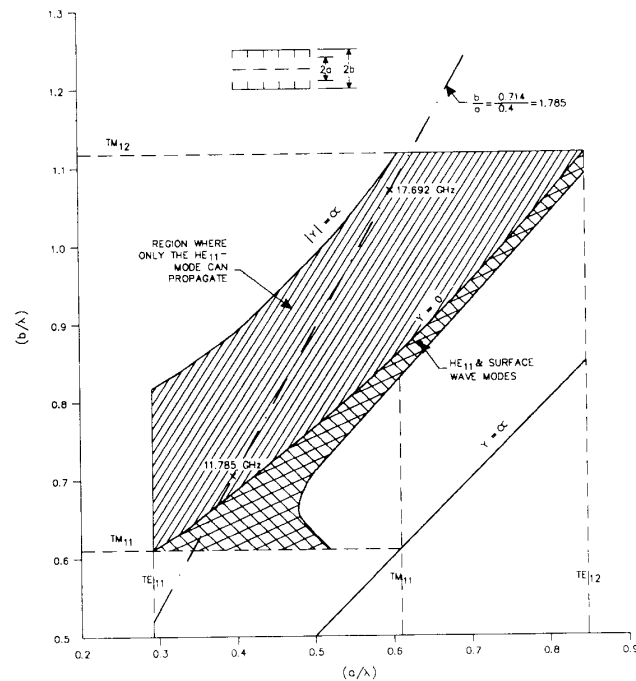


Fig. 1. Mode chart of a corrugated circular waveguide. The region where HE_{11} mode only can propagate is shown.

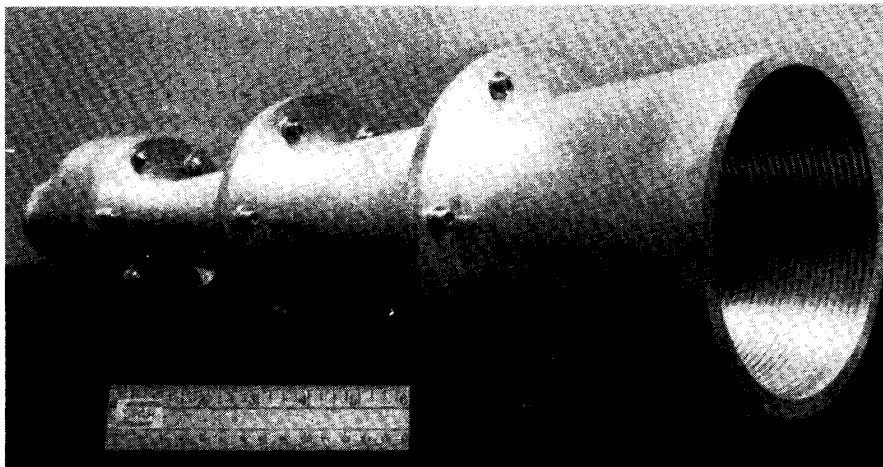


Fig. 2. Photograph of the corrugated horn showing the corrugations. The horn is fabricated in three different sections.

is varying) of the horn are fabricated using circular disks that are bolted together at the outer rim. The horn is fabricated in three sections with flange attachments. Figs. 2 and 3 show details of the horn fabricated.

III. EXPERIMENTAL RESULTS

The radiation patterns of the corrugated horn are measured in an anechoic chamber. The axis of rotation of the horn is made to coincide with the phase center location (varies with frequency) which is calculated using earlier formulations [10]–[12]. Measured co-pol and x-pol patterns at center frequencies of transmit and receive bands are shown in Figs. 4 and 5. Co-polar patterns shown in the figures

are measured in the E -plane, H -plane and 45° plane of the horn while the x-pol is measured in the 45° plane. The co-pol patterns in Figs. 4 and 5 are circularly symmetric and peak cross-polar levels are better than -39 and -34 dB (relative to peak) for the transmit and receive bands, respectively. Table I summarizes the measured results of the horn patterns. The x-pol values shown in Table I are the average of the peak values measured on either side of the boresight.¹ Additional

¹ The asymmetry in the cross-polar patterns shown in Figs. 4 and 5 is due to specular reflections from the range (seen on left half of the patterns). This has been verified by rotating the test horn by 180° and remeasuring the patterns. The cross-polar patterns remain unchanged indicating that the horn patterns are quite symmetrical. The cross-polar levels of the horn are expected to be marginally better than the measured average values shown in Table I.

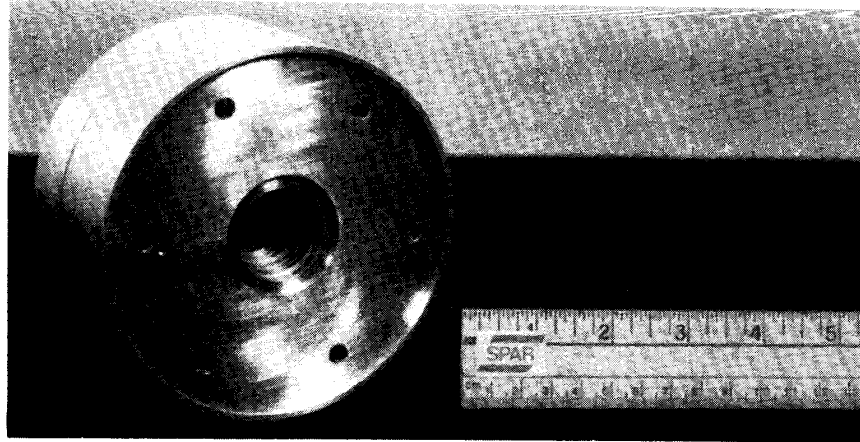


Fig. 3. Photograph of the input matching section of the horn.

TABLE I
SUMMARY OF MEASURED PATTERN RESULTS OF THE CORRUGATED HORN AT TRANSMIT AND RECEIVE BANDS

Frequency (GHz)	10 dB Beamwidth (Degrees)	Cross-Pol Peak in the 45° Plane Relative to Co-Pol Peak (dB)
11.77	10.58	-40.50
11.94	10.40	-39.50
12.11	10.33	-40.10
17.37	7.35	-36.25
17.54	7.20	-34.25
17.71	7.10	-34.50

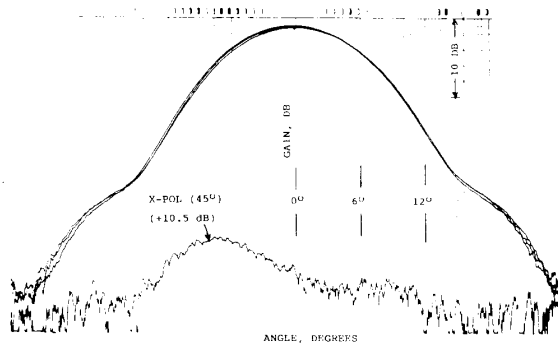


Fig. 4. Measured far-field patterns of the corrugated horn at 11.94 GHz frequency (center of the transmit band). Co-pol patterns are measured in E -, H -, and 45° planes while the cross-pol patterns are measured in the 45° plane.

measurements carried out covering the 11.0 GHz to 18.0 GHz (50% bandwidth) showed that the x-pol performance of the horn is better than -32 dB relative to peak and better than -34 dB in the desired frequency bands.

The return loss of the horn, measured over the required band, has improved from 23.5 to 28.3 dB with the addition of the input matching transformer section. Horn gain is measured as 24.8 and 27.98 dBi at 11.94 and 17.54 GHz, respectively.

IV. THEORETICAL RESULTS

The radiation patterns of the horn are calculated by integrating the aperture fields of the horn. The co- and cross-polar patterns of the

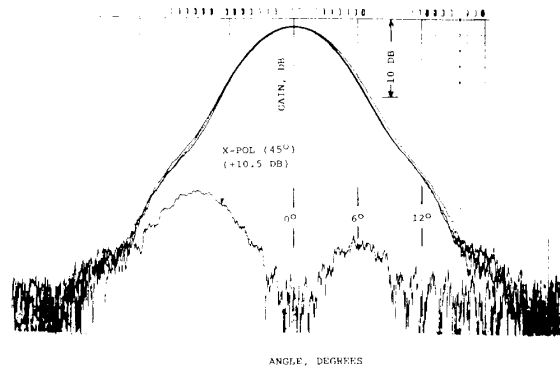


Fig. 5. Measured far-field patterns of the corrugated horn at 17.54 GHz frequency (center of the receive band). Co-pol patterns are measured in E -, H -, and 45° planes while the cross-pol patterns are measured in the 45° plane.

horn are given as [13]

$$E_{CP} = C[X_1 + VX_2 \cos(2\phi)] \tag{2}$$

$$E_{XP} = C \cdot V \cdot X_2 \sin(2\phi) \tag{3}$$

where

$$X_{1,2} = \int_0^1 J_{0,2}(Sr) \cdot J_{0,2}(ka \sin \Theta r) \exp \left[-j \frac{\pi a^2}{\lambda} \left(\frac{1}{L} + \frac{1}{R} \right) r^2 \right] dr \tag{4}$$

and

$$v = J_0(S)/J_2(S). \tag{5}$$

In the above equations a is the aperture radius, r is the normalized distance, L is the axial length of the horn, k is the face-space wavenumber ($k = 2\pi/\lambda$), R is the observations distance, $J_n(X)$ is

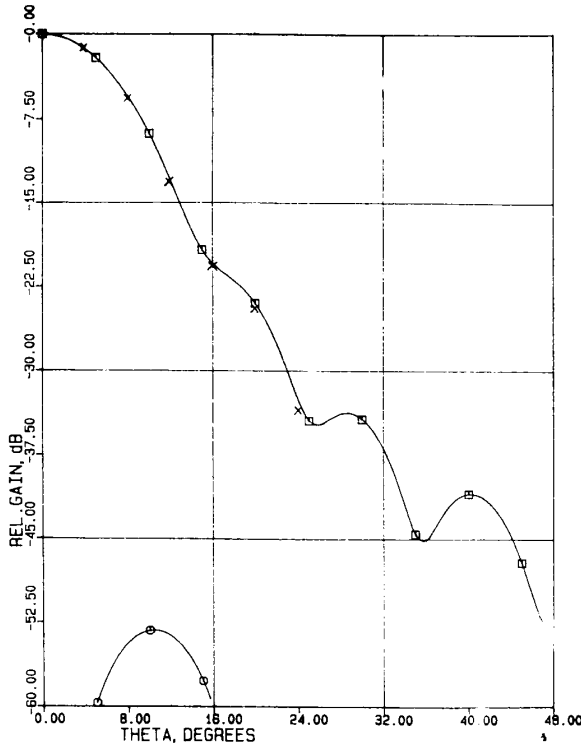


Fig. 6. Comparison between the computed and measured far-field patterns of the horn in 45° plane. Frequency is 11.94 GHz. □-□—co-pol pattern (computed); X-X—co-pol pattern (measured); O-O— x-pol pattern (computed).

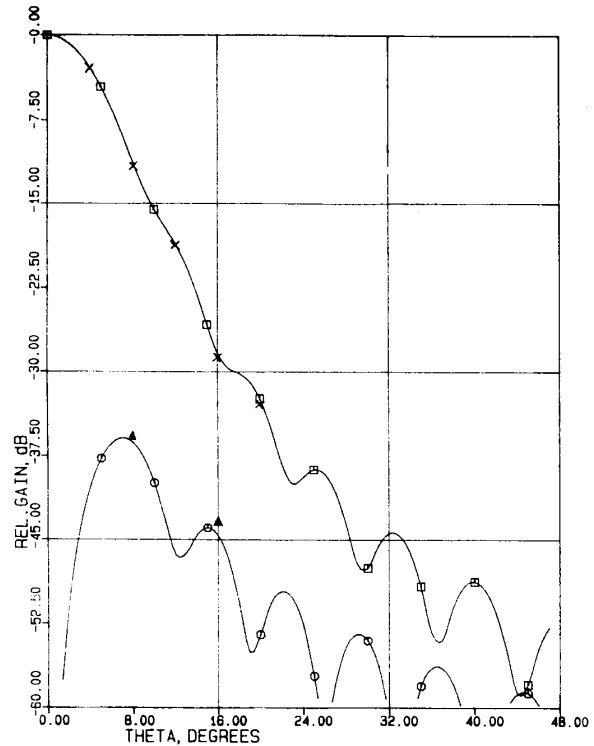


Fig. 7. Comparison between the computed and measured far-field patterns of the horn in the 45° plane. Frequency is 17.54 GHz. □-□—co-pol pattern (computed); X-X—co-pol pattern (measured); O-O— x-pol pattern (computed).

the Bessel function of first kind of order n and ϕ is the azimuth angle. The quadratic phase term in (4) is expressed in such a way that the formulation gives correct results in the Fraunhofer region ($R \rightarrow \infty$) as well as the Fresnel region [14]. The eigenvalue “ S ” associated with the hybrid mode is evaluated using the eigenvalue equation

$$\frac{J_1(S)}{S^3 J_1'(S)} \left[\left(\frac{S J_1'(S)}{J_1(S)} \right)^2 - 1 + \left(\frac{S}{ka} \right)^2 \right] + \frac{1}{\left(1 - \frac{t}{h} \right) \cdot ka \cdot \tan(kl)} = 0. \quad (6)$$

The range of S for the dominant hybrid mode is $1.841 \leq S \leq 2.405$. Figs. 6 and 7 show the computed co-pol and cross-pol patterns of the horns at center frequencies of the transmit and receive bands. They are calculated in the diagonal plane of the horn ($\phi = 45^\circ$). Measured co-pol data is shown in the figures for comparison. The cross-pol predictions are close to measurements at receive frequencies while there are some discrepancies at transmit band.

V. CONCLUSION

It is shown that single depth corrugated horn performance can be optimized to give low cross-polarization fields over a 40 percent frequency bandwidth. Cross-polar levels of the order -34 dB and return loss of better than 28 dB have been realized for the bread-board horn. The designed horn has potential application in the direct broadcast satellite antennas operating in the 12 and 17.5 GHz frequencies.

ACKNOWLEDGMENT

The author is thankful to Dr. K. K. Chan, Chan Technologies Incorporated, for his suggestions on the matching transformer for the horn.

REFERENCES

- [1] E. Carpenter, "A dual-band corrugated feed horn," in *Proc. IEEE Antennas Propagat. Symp.*, vol. 1, 1980, pp. 213-216.
- [2] S. Ghosh, "A corrugated waveguide feed for discrete multi-band applications having depth corrugations," in *Proc. IEEE Antennas Propagat. Symp.*, vol. 1, 1980, pp. 217-220.
- [3] S. Ghosh, N. Adatia, and B. K. Watson, "Hybrid-mode feed for multi-band applications having a dual-depth corrugation boundary," *Electron. Lett.*, vol. 18, no. 20, pp. 860-862, Sept. 30, 1982.
- [4] Y. Takeichi, T. Hashimoto, and F. Takeda, "The ring-loaded corrugated waveguide," *IEEE Trans. Microwave Theory Tech.*, vol. MTT-19, pp. 947-950, Dec. 1971.
- [5] F. Takeda and T. Hashimoto, "Broadbanding of corrugated conical horns by means of ring-loaded corrugated waveguide structure," *IEEE Trans. Antennas Propagat.*, vol. AP-24, no. 6, pp. 786-792, Nov. 1976.
- [6] C. Dragone and W. E. Legg, "Quarter-wave corrugated transformer for broadband matching of a corrugated feed," *AT&T Bell Labs. Tech. J.*, vol. 63, no. 2, pp. 207-215, Feb. 1984.
- [7] B. M. Thomas, "Design of corrugated conical horns," *IEEE Trans. Antennas Propagat.*, vol. AP-26, no. 2, pp. 367-372, Mar. 1978.
- [8] P. J. B. Clarricoats *et al.*, "Optimum design of corrugated feeds for low cross-polar radiation," in *Proc. European Microwave Conf.*, vol. 6, 1976, pp. 148-152.
- [9] B. M. Thomas, "Mode conversion using circumferentially, corrugated cylindrical waveguide," *Electron. Lett.*, vol. 8, pp. 394-396, 1972.
- [10] P. S. Kildal, "Gaussian beam model for aperture-controlled and flare-angle-controlled corrugated horn antennas," *Inst. Elec. Eng. Proc.*, vol. 135, pt. H, no. 4, pp. 237-240, Aug. 1988.